NASA/TP—2011–216461

An Estimate of the Size and Shape of Sunspot Cycle 24 Based on Its Early Cycle Behavior Using the Hathaway-Wilson-Reichmann Shape-Fitting Function

Robert M. Wilson
Marshall Space Flight Center, Marshall Space Flight Center, Alabama

March 2011

The NASA STI Program…in Profile

Since its founding, NASA has been dedicated to the advancement of aeronautics and space science. The NASA Scientific and Technical Information (STI) Program Office plays a key part in helping NASA maintain this important role.

The NASA STI Program Office is operated by Langley Research Center, the lead center for NASA's scientific and technical information. The NASA STI Program Office provides access to the NASA STI Database, the largest collection of aeronautical and space science STI in the world. The Program Office is also NASA's institutional mechanism for disseminating the results of its research and development activities. These results are published by NASA in the NASA STI Report Series, which includes the following report types:

- TECHNICAL PUBLICATION. Reports of completed research or a major significant phase of research that present the results of NASA programs and include extensive data or theoretical analysis. Includes compilations of significant scientific and technical data and information deemed to be of continuing reference value. NASA's counterpart of peer-reviewed formal professional papers but has less stringent limitations on manuscript length and extent of graphic presentations.

- TECHNICAL MEMORANDUM. Scientific and technical findings that are preliminary or of specialized interest, e.g., quick release reports, working papers, and bibliographies that contain minimal annotation. Does not contain extensive analysis.

- CONTRACTOR REPORT. Scientific and technical findings by NASA-sponsored contractors and grantees.

- CONFERENCE PUBLICATION. Collected papers from scientific and technical conferences, symposia, seminars, or other meetings sponsored or cosponsored by NASA.

- SPECIAL PUBLICATION. Scientific, technical, or historical information from NASA programs, projects, and mission, often concerned with subjects having substantial public interest.

- TECHNICAL TRANSLATION. English-language translations of foreign scientific and technical material pertinent to NASA's mission.

Specialized services that complement the STI Program Office's diverse offerings include creating custom thesauri, building customized databases, organizing and publishing research results…even providing videos.

For more information about the NASA STI Program Office, see the following:

- Access the NASA STI program home page at <http://www.sti.nasa.gov>

- E-mail your question via the Internet to <help@sti.nasa.gov>

- Fax your question to the NASA STI Help Desk at 443–757–5803

- Phone the NASA STI Help Desk at 443–757–5802

- Write to:
  NASA STI Help Desk
  NASA Center for AeroSpace Information
  7115 Standard Drive
  Hanover, MD 21076–1320

NASA/TP—2011–216461

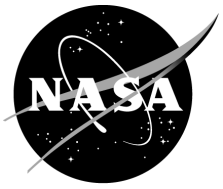

An Estimate of the Size and Shape of Sunspot Cycle 24 Based on Its Early Cycle Behavior Using the Hathaway-Wilson-Reichmann Shape-Fitting Function

Robert M. Wilson
Marshall Space Flight Center, Marshall Space Flight Center, Alabama

National Aeronautics and
Space Administration

Marshall Space Flight Center • MSFC, Alabama 35812

March 2011

Available from:

NASA Center for AeroSpace Information
7115 Standard Drive
Hanover, MD 21076–1320
443–757–5802

This report is also available in electronic form at
<https://www2.sti.nasa.gov/login/wt/>

TABLE OF CONTENTS

LIST OF FIGURES

LIST OF TABLES

LIST OF ACRONYMS AND ABBREVIATIONS

12-mma	12-month moving average
aam	minimum value of the 12-mma of the aa-geomagnetic index
ASC	ascent duration
<ASC>	mean cycle ascent duration
E(Rm)	epoch of minimum amplitude occurrence
E(ΔR(*t*) max)	epoch of maximum month-to-month rate of change in R(*t*)
fd	first difference (same as ΔR(*t*))
FRC	fast-rising cycle
HWR	Hathaway-Wilson-Reichmann
J	January
LPC	long-period cycle
PER	period
<PER>	mean cycle period
R	monthly mean sunspot number
RM	maximum amplitude
<RM>	mean cycle maximum amplitude
Rm	minimum amplitude
R(*t*)	12-mma of monthly mean sunspot number at elapsed time *t*
ΔR(*t*)	month-to-month change in R(*t*)
ΔR(*t*) max	maximum month-to-month rate of change in R(*t*)
SCN	sunspot cycle number
SPC	short-period cycle
SRC	slow-rising cycle
TP	Technical Publication

NOMENCLATURE

a	parameter in HWR shape-fitting function; also the y-intercept in the regression equation
ad	average deviation
b	parameter in HWR shape-fitting function; also the slope in the regression equation
c	parameter in HWR shape-fitting function
cl	confidence level
P	probability
r	coefficient of correlation
r^2	coefficient of determination
se	standard error of estimate
t	elapse time in months from E(Rm) to E(R(t))
t_0	initial starting point
x	independent variable in regression equation
y	dependent variable in regression equation
y'	alternate dependent variable in the regression equation

TECHNICAL PUBLICATION

AN ESTIMATE OF THE SIZE AND SHAPE OF SUNSPOT CYCLE 24 BASED ON ITS EARLY CYCLE BEHAVIOR USING THE HATHAWAY-WILSON-REICHMANN SHAPE-FITTING FUNCTION

1. INTRODUCTION

Having a reliable estimate for the strength and duration of solar activity over the course of the solar cycle is important for a variety of reasons. Namely, it provides a decadal overview of the expected space weather conditions that likely will prevail years in advance, which is important for planning space missions to the moon, asteroids, and planets, and which also is important for climatology, electrical power distribution, and global communication. Additionally, it possibly can provide an early indication for establishing the start, end, or continuance of a suspected long-term anomalous trend in solar activity (e.g., a continuing secular rise or fall, or the occurrence of another Maunder- or Dalton-like minimum or a Grand- or Modern-like maximum).[1–15]

In this Technical Publication (TP), the very early solar/geomagnetic activity of cycle 24 is examined to ascertain the likely level of solar activity over the remainder of the solar cycle. In particular, (1) 12-month moving averages (12-mma) of monthly mean sunspot number (R) for cycle 24 are compared against 12-mma values for the mean of cycles 10–23 (the modern sunspot era); (2) its maximum month-to-month rate of rise ($\Delta R(t)$ max), as observed thus far, is compared to the maximum month-to-month rate of rise for the mean cycle;[16] (3) the minimum amplitude of the 12-mma aa-geomagnetic index (aam) for cycle 24 is compared against those for other sunspot cycles; (4) the method of Ohl[17–22] is used to predict the expected maximum amplitude (RM) for cycle 24; (5) the Waldmeier effect[23,24] is used to estimate the ascent duration (ASC) (i.e., the elapsed time between minimum and maximum amplitude occurrences) for cycle 24; (6) 12-mma averages of monthly mean sunspot number are compared against 12-mma mean values for selected groupings of sunspot cycles (e.g., slow- and fast-rising cycles and long- and short-period cycles); and (7) 12-mma values of monthly mean sunspot number are compared against selected Hathaway-Wilson-Reichmann (HWR) shape-fitting functions[25] to determine the best fit for the very early behavior of cycle 24.

2. RESULTS

Figure 1 shows (a) R(t) for cycle 24 (the filled circles, elapsed time t = 0–18 mo) and those for the mean modern era sunspot cycle (the smoothed line, t = 0–60 mo, based on an epoch analysis of cycles 10–23 using minimum amplitude occurrence as the common epoch for comparison), (b) the ratio of cycle 24 R(t) values to those of the mean modern era sunspot cycle, and (c) the month-to-month rate of rise (ΔR(t)) using the 12-mma values of cycle 24 and the mean modern era sunspot cycle. Also shown are RM, ASC, ΔR(t) max, and E(ΔR(t) max) for the modern era sunspot cycles. Clearly, cycle 14 is the smallest modern era sunspot cycle (RM = 64.2) yet observed, while cycle 19 is the largest (201.3). Also, cycle 12 is the slowest rising modern era sunspot cycle (ASC = 60 mo) yet observed, while cycle 22 is the fastest rising (34 mo). Of the 14 modern era sunspot cycles, 7 have had RM ≤110.6 (cycle 20) and 8 have had ASC ≤47 mo (cycles 19 and 23).

Regarding ΔR(t) max, cycle 14 has the smallest maximum month-to-month rate of rise (3.9) yet observed, while cycle 19 has the largest (10.8). Cycle 12 has the earliest occurring ΔR(t) max (14 mo) yet observed, while cycle 15 has the latest occurring ΔR(t) max (42 mo). Of the 14 modern era sunspot cycles, 8 have had ΔR(t) max ≤6.4 (cycles 17 and 20), 7 have had ΔR(t) max occurring between 14 and 24 mo, and 7 have had ΔR(t) max occurring between 30 and 42 mo.

Thus far, R(t) values for cycle 24 have remained well below that of the mean modern era sunspot cycle, having a ratio against the mean cycle (R(t) cycle 24 to R(t) mean cycle) <0.5, inferring that, if this ratio continues through the occurrence of maximum amplitude, RM for cycle 24 will be <60. Likewise, the maximum ΔR(t) yet observed for cycle 24 has remained ≤1.7, a rate less than half the maximum month-to-month rate of rise observed for cycle 14 (3.9), the smallest cycle of the modern era. Together, these observations suggest that cycle 24 potentially might become the new smallest cycle of the modern era,[26] and, possibly herald the occurrence of another Maunder- or Dalton-like minimum.

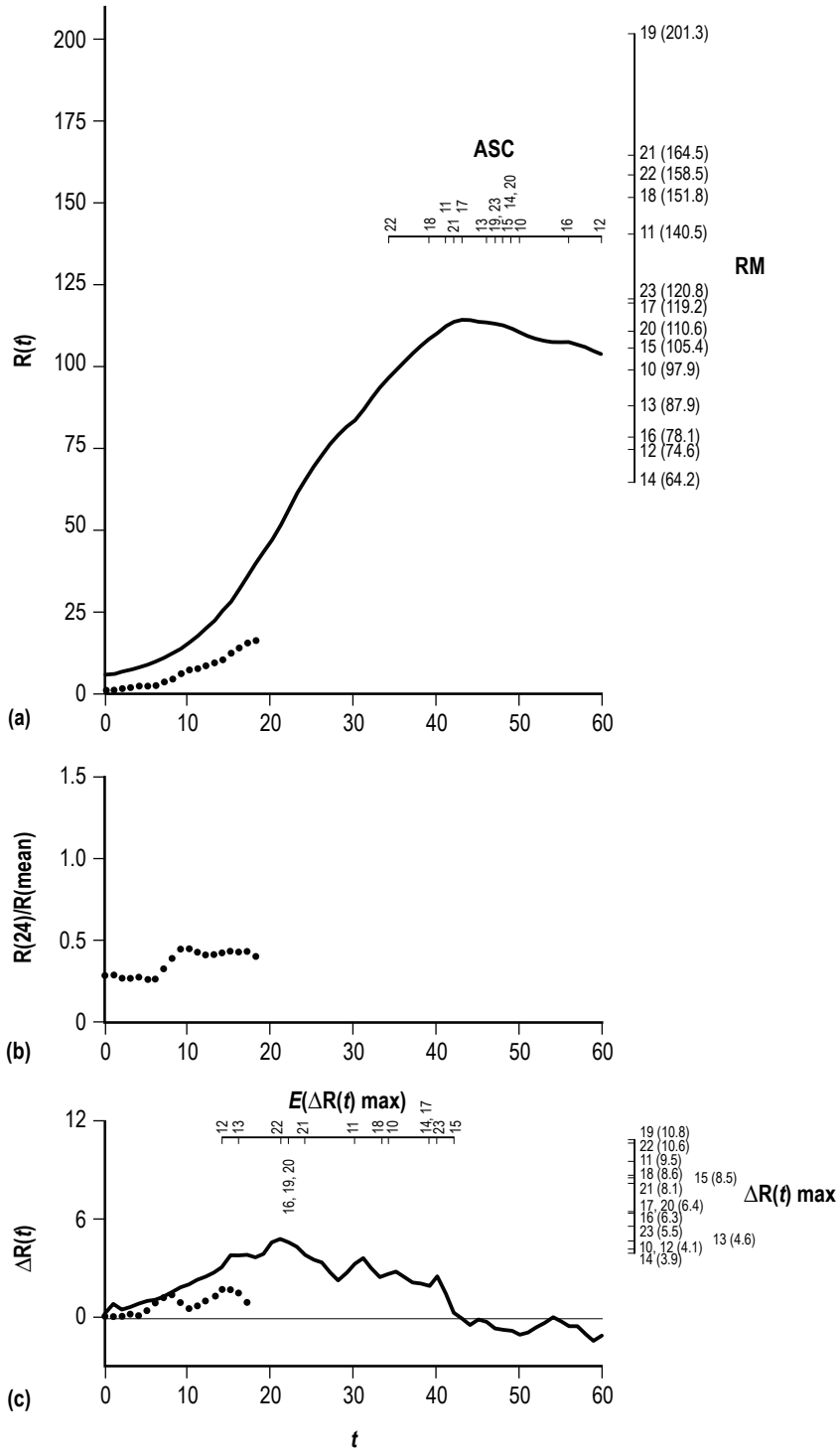

Figure 1. Variation of (a) 12-mma values of R(t) for cycle 24 (t = 0–18) and the mean modern era sunspot cycle (t = 0–60); (b) the ratio of R(t) cycle 24 values to mean modern era sunspot cycle values; and (c) variation of ΔR(t) values for cycle 24 and the mean modern era sunspot cycle.

Figure 2 depicts RM versus $\Delta R(t)$ max for the modern era sunspot cycles, where $\Delta R(t)$ max is the maximum rate of growth in R during the ascending phase of the sunspot cycle ($\Delta R(t)$ max for cycle 14 actually is 4.5; however, this value occurred after the occurrence of its maximum amplitude). A strong preferential linear correlation is indicated, one having a coefficient of correlation $r = 0.86$, a standard error of estimate $se = 21.3$, and a confidence level $cl > 99.9\%$ for the inferred regression. The inferred regression equation is $y = 22.041 + 14.032x$, where y represents RM and x represents $\Delta R(t)$ max, and the inferred regression can explain about 73% of the variance in RM (i.e., the coefficient of determination $r^2 = 0.73$). For cycle 24, because the maximum value for $\Delta R(t)$ is presently only 1.7 (through $t = 18$ mo), one infers cycle 24's RM = 45.9 ± 21.3 (the ±1 *se* prediction interval). Clearly, however, since t has only recently entered the window when one expects to find $\Delta R(t)$ max ($t \geq 14$ mo), one can not know with complete certainty that $\Delta R(t)$ max for cycle 24 has indeed been observed. The value of 1.7 could easily be exceeded in the coming months, which, if true, would indicate a higher RM for cycle 24. Fisher's exact test[27] for 2×2 contingency tables shows that the probability of obtaining the observed result (6:1:5:2), or one more suggestive of a departure from independence, is $P = 5.1\%$. Thus, RM for cycle 24 is expected to lie within the lower-left quadrant (i.e., RM < 114.9) if $\Delta R(t)$ max <6.4. (In fig. 2 and succeeding figs. 3–5 and 8, filled circles denote slow-rising, long-period cycles—those having ASC ≥48 mo and PER ≥132 mo; unfilled circles denote fast-rising, long-period cycles; filled triangles denote slow-rising, short-period cycles; and unfilled triangles denote fast-rising, short-period cycles.)

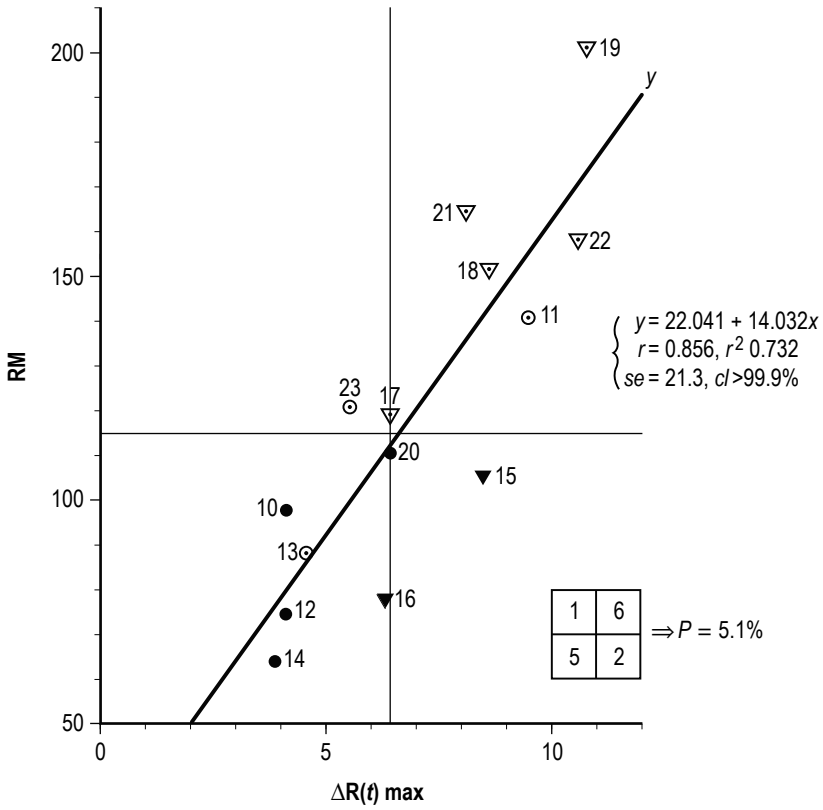

Figure 2. RM versus $\Delta R(t)$ max.

Figure 3 shows the cyclic variation of (a) RM and (b) the minimum value of the 12-mma aa-geomagnetic index (aam) for the modern era sunspot cycle, where SCN refers to the sunspot cycle number. Noticeable is a seemingly strong preferential behavioral correlation between RM and aam, one depicting a rise in the level of solar activity between cycles 14 and 19, a dip in cycle 20, resurgence in cycle 21, and a decline thereafter. The horizontal lines denote the parametric medians and the unfilled box (cycle 24) simply denotes that presently the nature of cycle 24 remains unknown (i.e., whether its ASC is one typical of fast- or slow-rising cycles and whether its PER is one typical of long- or short-period cycles). While true, because of the inferred closely correlated behavior between RM and aam, one strongly suspects that cycle 24 will have RM below the median (114.9), being of similar size to early cycles 12 and 14.

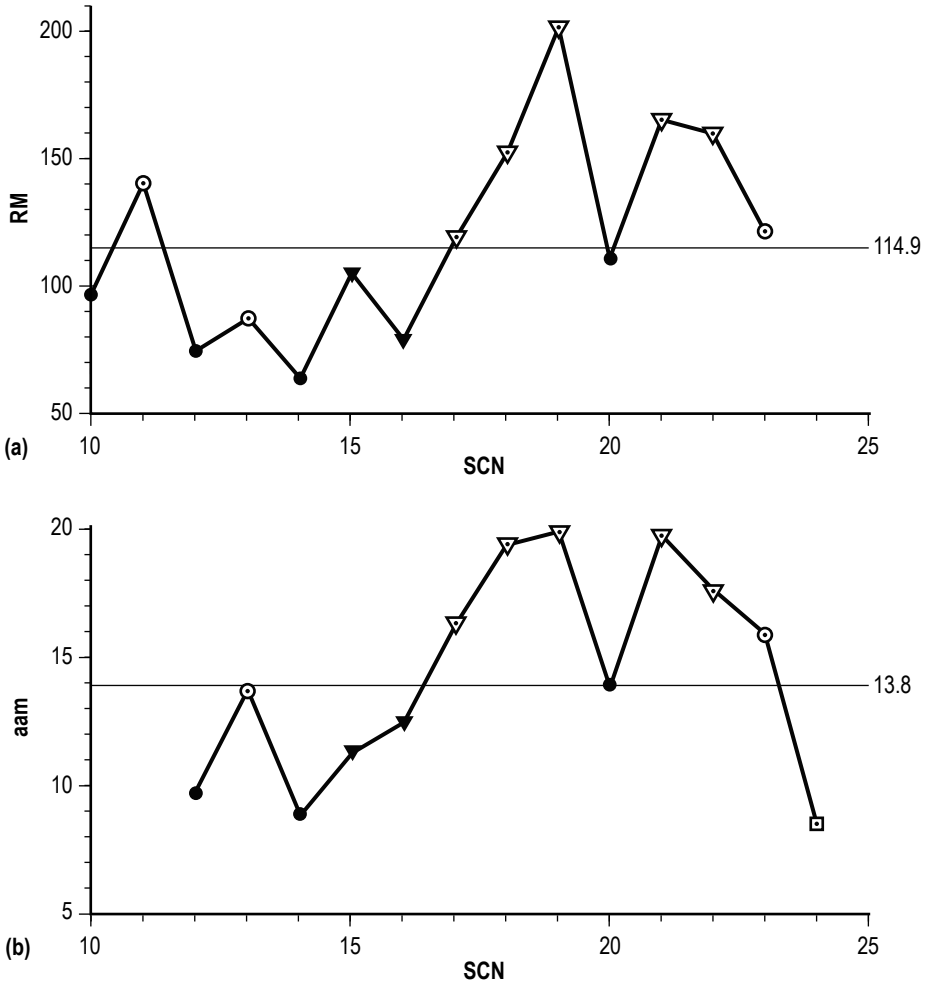

Figure 3. Variation of (a) RM and (b) aam for cycles 12–24.

Figure 4 compares RM and aam for cycles 12–23, the so-called method of Ohl. Some 40 years ago, Ohl[17,18] noted that the minimum level of geomagnetic activity in the vicinity of sunspot cycle minimum amplitude (Rm) occurrence provides a simple means for estimating the later occurring expected size (maximum amplitude RM) of the ongoing sunspot cycle, usually about 3 years in advance. The observed scatter plot suggests a very strong preferential linear relationship between RM and aam, one having $r = 0.93$ and $se = 16.6$. Hence, given the value of aam for a sunspot cycle, one can infer its expected size usually to within about 11%, on average. For cycle 24, its observed aam value of 8.4 (the lowest on record, denoted by the downward-pointing arrow along the x-axis and occurring at $t = 8$ and 9 mo past E(Rm)) suggests $RM = 54.6 \pm 16.6$ (based on the inferred regression), 54.6 ± 12.8 (based on the average deviation, *ad*), or 54.6 ± 6 (based on the 11% average percentage of deviation; the maximum observed percentage of deviation for the modern era sunspot cycles is about 22%). From the inferred regression, one finds that there is only a 1% chance that RM for cycle 24 will exceed 100.5. Hence, RM for cycle 24 very probably will lie within the lower-left quadrant of figure 4, unless, of course, cycle 24 should turn out to be a statistical outlier. (It should be noted that aam usually occurs between $t = 0$–8 mo following E(Rm), true for 7 of 12 sunspot cycles, including cycles 12, 13, 15, 17, 20, and 21; only cycle 14 had its aam prior to E(Rm), having occurred at $t = -8$, –5, and –4 mo, and cycles 16, 18, 19, and 23 had a later occurring aam, at $t = 12$ –17 mo.)

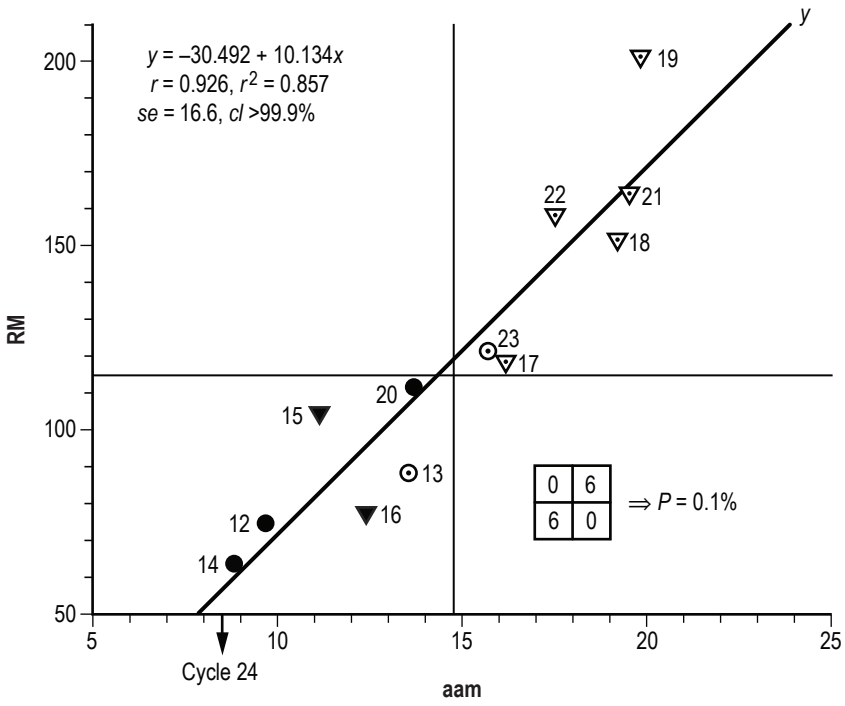

Figure 4. RM versus aam (the method of Ohl).

Figure 5 depicts the scatter plot of ASC versus RM, demonstrating the so-called Waldmeier effect.[23,24] Namely, stronger cycles tend to rise to maximum amplitude more quickly than weaker cycles. Based on the observed 2×2 contingency table, the probability of obtaining the observed

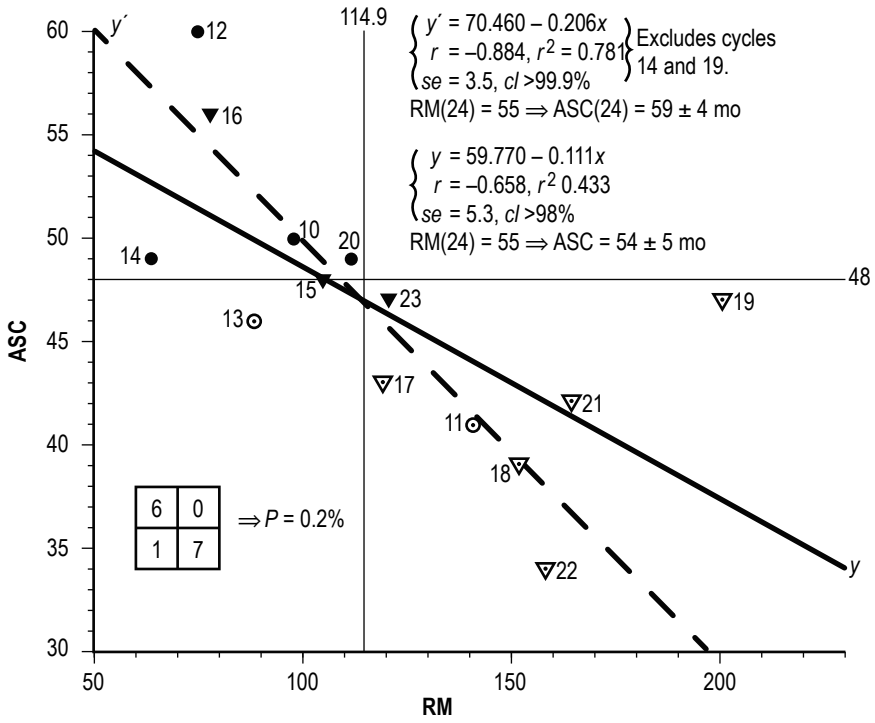

Figure 5. ASC versus RM (the Waldmeier effect).

result, or one more suggestive of a departure from independence, is $P = 0.2\%$ (from Fisher's exact test for 2×2 contingency tables). Hence, a sunspot cycle having RM <114.9 is strongly expected to have ASC ≥48 mo. Because the predicted value for cycle 24's RM is <114.9 (based on the method of Ohl), it follows that one expects cycle 24 to be a slow-rising cycle (i.e., ASC ≥48 mo), inferring E(RM) for cycle 24 after December 2012.

Also shown in figure 5 are two inferred regression lines, one using all modern era sunspot cycles (y) and the other using all modern era sunspot cycles except the extremes (y', cycles 14 and 19). Based on the predicted value of RM = 55, one infers ASC = 54 ± 5 (using y) or ASC = 59 ± 4 (using y') for cycle 24. Hence, cycle 24's RM is expected to occur sometime in 2013 to early 2014 (the prediction intervals are ±1 *se*.)

Table 1 summarizes hindcasts of RM and ASC based on the method of Ohl and the Waldmeier effect. Given in the table are the observed values of aam, RM, and ASC for cycles 12–23 and the aam value for cycle 24. The predicted value of RM is deduced using the inferred preferential regression from the method of Ohl (fig. 4). The predicted value of ASC is deduced using the inferred preferential regression from the Waldmeier effect (y, fig. 5) based on the predicted value of RM from the method of Ohl. The differences (observed minus predicted) are identified for both RM and ASC. The average deviation (*ad*) appears at the bottom of the differences.

Table 1. Hindcasts of RM and ASC based on inferred estimates.

	Observed			Predicted		Differences	
Cycle	aam	RM	ASC	RM	ASC	RM	ASC
12	9.7	74.6	60	67.8	52	6.8	8
13	13.6	87.9	46	107.3	48	–19.4	–2
14	8.9	64.2	49	59.7	53	4.5	–4
15	11.2	105.4	48	83.0	51	22.4	–3
16	12.4	78.1	56	95.2	49	–17.1	7
17	16.2	119.2	43	133.7	45	–14.5	–2
18	19.3	151.8	39	165.1	41	–13.3	–2
19	19.9	201.3	47	171.2	41	30.1	6
20	13.8	110.6	49	109.4	48	1.2	1
21	19.6	164.5	42	168.1	41	–3.6	1
22	17.5	158.5	34	146.9	43	11.6	–9
23	15.8	120.8	47	129.6	45	–8.8	2
24	8.4	–	–	54.6	54	–	–
					ad	12.8	4

Figure 6 compares the observed early rise of cycle 24 (the filled circles) with the mean of (a) fast-rising cycles (FRC), (b) slow-rising cycles (SRC), (c) short-period cycles (SPC), and (d) long-period cycles (LPC), where the means are computed for $t = 0$–36 mo using E(Rm) as the common epoch for comparison. Also given in subpanels (a)–(d) are the mean values of RM, ASC, and PER for each grouping of sunspot cycles. Hence, for the FRC group, on average, $\langle RM \rangle = 144 \pm 34$, $\langle ASC \rangle = 42 \pm 4$ mo, and $\langle PER \rangle = 131 \pm 12$ mo (± 1 *se* prediction intervals). For the SRC group, the means are, respectively, about 89 ± 19, 52 ± 5, and 132 ± 9; for the SPC group, the means are, respectively, about 140 ± 41, 44 ± 7, and 122 ± 3; and for the LPC group, the means are, respectively, about 100 ± 27, 49 ± 6, and 140 ± 5. Noticeable is that the R values for cycle 24 have remained well below the monthly means of all cycle groupings for $t = 0$–18 mo, inferring that RM for cycle 24 very likely will be far smaller than indicated by the group cycle means.

Table 2 gives the ratios of R(t) values for cycle 24 to the mean cycle and to each grouping of sunspot cycles for $t = 0$–18 mo. As previously noted, in comparison to the mean cycle, cycle 24 is behaving as if its R(t) values will remain below 0.5, inferring that its RM will be <60. Compared to the FRC group, the ratio has remained below about 0.4, also inferring RM < 60. Similarly, for the other groups, SRC, SPC, and LPC, the ratios have remained below about 0.6, 0.4, and 0.5, respectively, inferring RM < 55. However, because ΔR(t) max probably has not yet been observed, one suspects that the ratios will become slightly larger, indicating a slightly higher predicted RM for cycle 24. Recall that first difference R(t) values (fd R(t)) have only recently entered the window when one finds ΔR(t) max ($t \geq 14$ mo), so the maximum rate of rise probably has not yet been seen. (The window extends from 14 to 42 mo, based on the modern era sunspot cycles, with the inflection point occurring, on average, about 28 mo past E(Rm); 7 of 14 inflection points have occurred between $t = 14$–24 mo and 10 of 14 inflection points have occurred between $t = 14$–34 mo, with only cycles 14, 15, 17 and 23 having maximum month-to-month rates of rise longer than 3 years past minimum amplitude.)

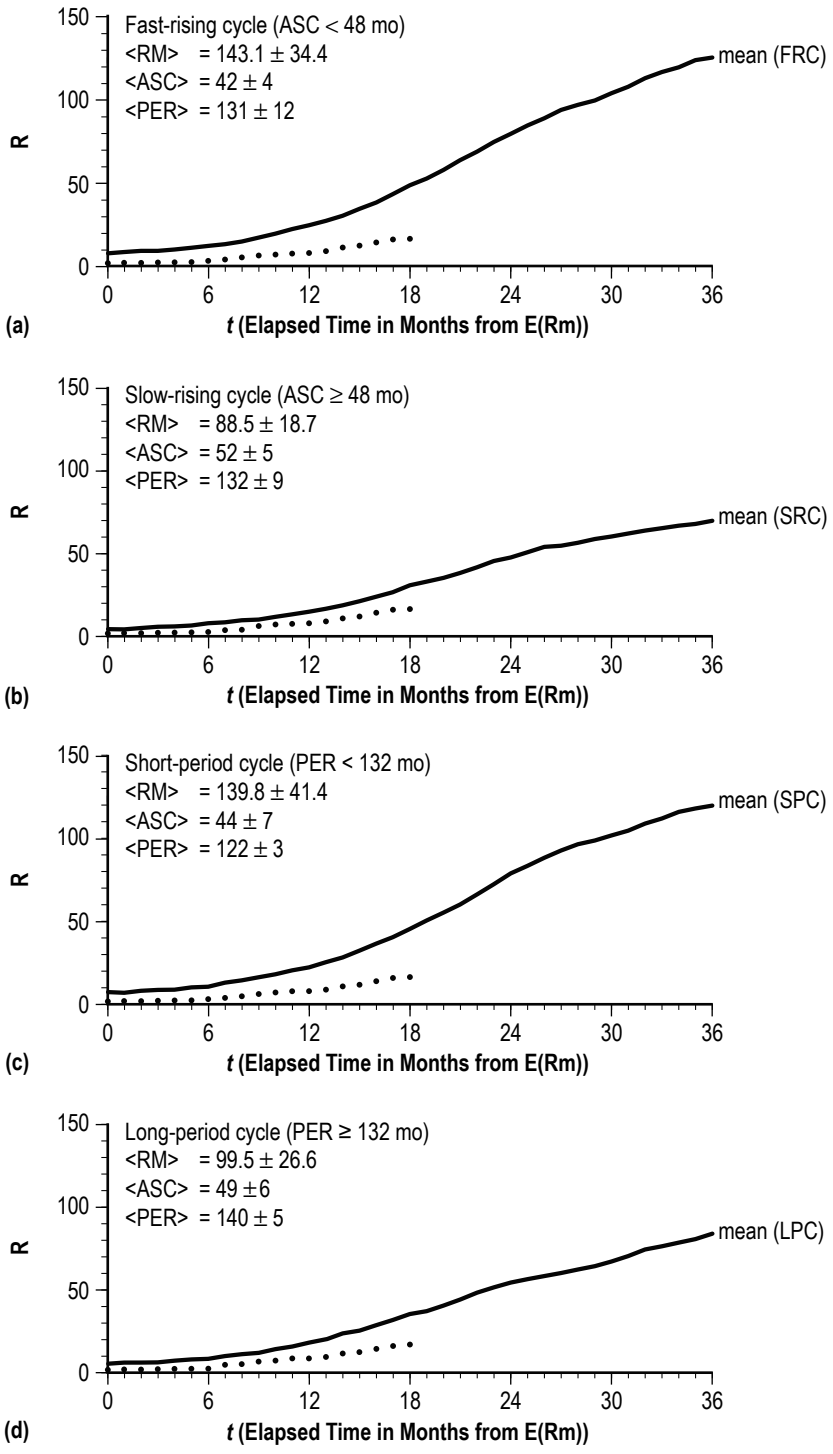

Figure 6. Comparison of 12-mma values of R(t) for cycle 24 and (a) the mean of fast-rising modern era sunspot cycles; (b) the mean of slow-rising modern era sunspot cycles; (c) the mean of short-period modern era sunspot cycles; and (d) the mean of long-period modern era sunspot cycles.

Table 2. Ratios of cycle 24 R(t) values to mean values for selected groupings of cycles for $t = 0$–18 mo.

t	Mean RM = 119.7	SRC RM = 88.5	FRC RM = 143.1	LPC RM = 99.5	SPC RM = 139.8
0	0.29	0.41	0.24	0.33	0.26
1	0.29	0.42	0.24	0.33	0.26
2	0.27	0.39	0.22	0.32	0.23
3	0.27	0.36	0.22	0.31	0.23
4	0.27	0.35	0.23	0.32	0.24
5	0.26	0.34	0.22	0.30	0.22
6	0.27	0.36	0.23	0.32	0.24
7	0.33	0.42	0.28	0.38	0.29
8	0.39	0.51	0.33	0.45	0.34
9	0.45	0.60	0.38	0.51	0.39
10	0.45	0.61	0.37	0.51	0.40
11	0.43	0.59	0.35	0.48	0.38
12	0.41	0.49	0.34	0.46	0.37
13	0.41	0.50	0.34	0.46	0.37
14	0.42	0.57	0.35	0.47	0.38
15	0.43	0.51	0.36	0.49	0.39
16	0.43	0.58	0.37	0.49	0.39
17	0.43	0.58	0.36	0.49	0.39
18	0.41	0.55	0.35	0.47	0.36

Previously, HWR[25] described a simple function, consisting of two parameters (RM and ASC), that appears to adequately reproduce the general shape (using sunspot number) of each sunspot cycle. The formulation (adapted for using 12-mma values of R) is

$$R(t) = a(t - t_0)^3 / \{\exp[(t - t_0)^2 / b^2] - c\} \quad , \tag{1}$$

where $a = (RM)b^{-3}/0.504$, $b = (ASC)/1.081$, $c = 0.71$, and t_0 is the initial starting point (E(Rm)). Using selected values of RM and ASC, one can generate numerous shapes for the sunspot cycle curve and compare them to actual values of R during the early rising phase of the sunspot cycle for a determination of the most appropriate fit.

Table 3 summarizes six cases that were examined for comparison to the early growth phase of cycle 24. The computed values using the HWR shape-fitting function extend 2 yr, although at the time of writing, R values for cycle 24 are known only $t = 18$ mo. The closest fit to cycle 24 values appears to be that of case 6, which uses RM = 70 and ASC = 56 mo.

Table 3. Comparison of predicted and observed R(t) values for cycle 24 using selected values of RM and ASC in the HWR shape-fitting function.

	R(t)(Predicted)						
t	Case 1	Case 2	Case 3	Case 4	Case 5	Case 6	R(t)(Observed)
0	0.0	0.0	0.0	0.0	0.0	0.0	1.7
1	0.0	0.0	0.0	0.0	0.0	0.0	1.8
2	0.0	0.0	0.0	0.0	0.0	0.0	1.9
3	0.1	0.0	0.1	0.1	0.1	0.1	2.0
4	0.1	0.1	0.2	0.1	0.3	0.2	2.2
5	0.3	0.2	0.4	0.3	0.5	0.4	2.3
6	0.4	0.3	0.6	0.5	0.9	0.7	2.7
7	0.7	0.5	1.0	0.8	1.4	1.1	3.6
8	1.0	0.7	1.4	1.1	2.0	1.6	4.8
9	1.4	1.0	2.0	1.5	2.8	2.3	6.2
10	1.8	1.3	2.6	2.1	3.7	3.0	7.1
11	2.4	1.7	3.4	2.7	4.8	4.0	7.6
12	3.0	2.2	4.3	3.4	6.1	5.0	8.3
13	3.7	2.7	5.3	4.2	7.5	6.2	9.3
14	4.5	3.3	6.5	5.1	9.1	7.5	10.6
15	5.3	3.9	7.7	6.1	10.7	8.9	12.3
16	6.3	4.6	9.0	7.2	12.6	10.5	14.0
17	7.3	5.4	10.4	8.4	14.5	12.2	15.5
18	8.3	6.2	11.9	9.7	16.5	13.9	16.4
19	9.4	7.1	13.5	11.0	18.7	15.8	–
20	10.6	8.0	15.1	12.4	20.9	17.7	–
21	11.7	9.0	16.8	13.8	23.1	19.7	–
22	13.0	10.0	18.5	15.3	25.4	21.8	–
23	14.2	11.0	20.2	16.9	27.8	23.9	–
24	15.5	12.1	22.0	18.4	30.1	26.1	–

Case 1: RM = 40 and ASC = 55 mo, implying a = 0.000603 and b = 50.8788 in the HWR fit
Case 2: RM = 40 and ASC = 62 mo, implying a = 0.000421 and b = 57.3543 in the HWR fit
Case 3: RM = 55 and ASC = 54 mo, implying a = 0.000875 and b = 49.9537 in the HWR fit
Case 4: RM = 55 and ASC = 59 mo, implying a = 0.000671 and b = 54.5791 in the HWR fit
Case 5: RM = 70 and ASC = 52 mo, implying a = 0.001248 and b = 48.1036 in the HWR fit
Case 6: RM = 70 and ASC = 56 mo, implying a = 0.000999 and b = 51.8039 in the HWR fit

Figure 7 depicts an initial projection for cycle 24 based on case 6 for t = 0–140 mo. The box spans 49–72 in terms of R(t) and 49–63 mo in terms of t, being based on predictions of RM and ASC for cycle 24 discussed earlier in the text. Thus, cycle 24 is expected to be at or near RM sometime between January 2013 and March 2014, being of comparable size to that of cycle 14. With the inclusion of additional observations of R over the next year or so, one should be able to significantly improve the projection of solar activity for the remainder of cycle 24. For example, determining the maximum rate of growth during the ascending phase of cycle 24 and determining exactly when it occurs relative to E(Rm) (the inflection point) should greatly improve the prediction of RM and the overall fit using the HWR shape-fitting function.

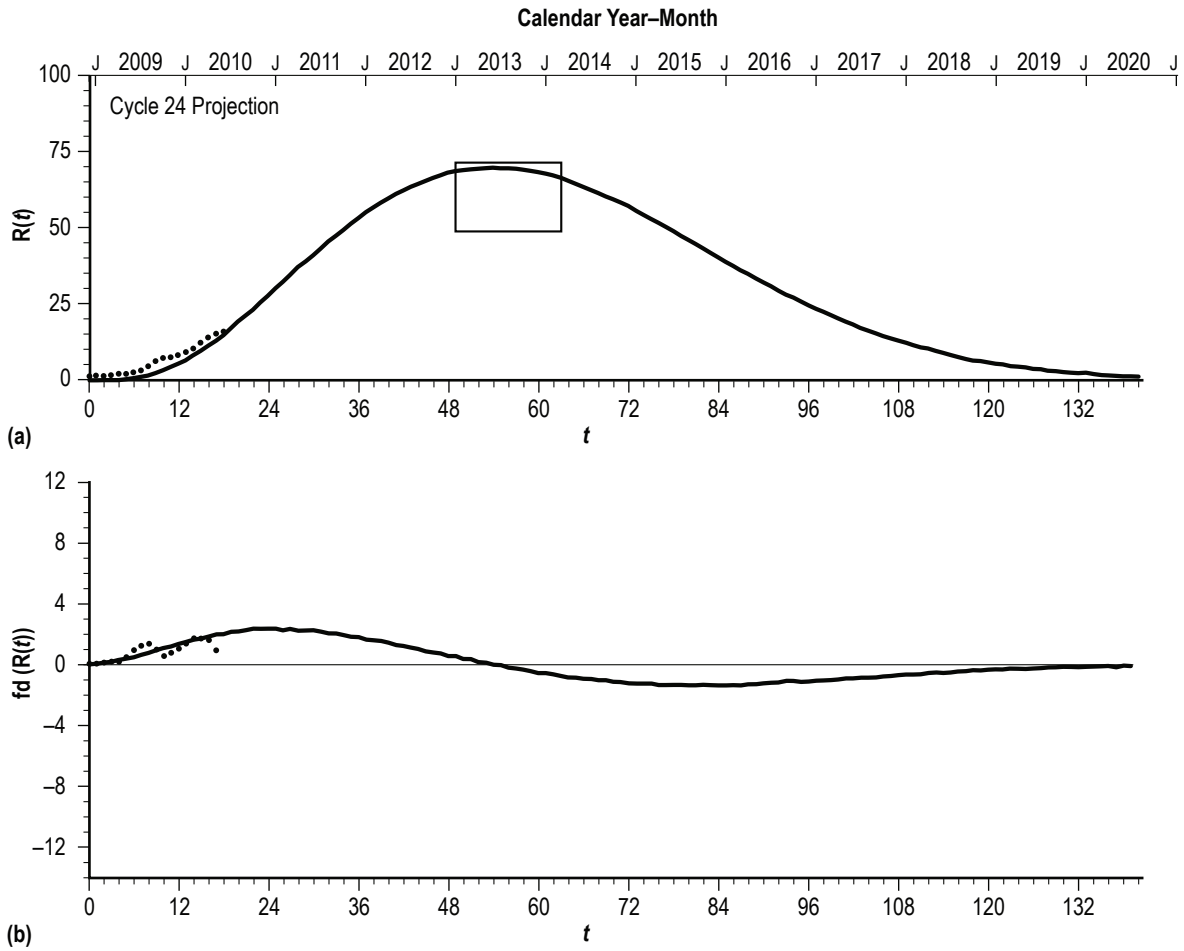

Figure 7. Values for cycle 24 and the HWR shape-fitting function using RM = 70 and ASC = 56: (a) Comparison of 12-mma values and (b) comparison of the fd (R(*t*)).

Previously, Wilson and Hathaway[16] examined various aspects of using the inflection point during the ascending phase to determine predictions of the size and timing of maximum amplitude for sunspot cycles. In particular, they noted that a highly statistically significant association exists between RM and the slope of the line drawn between E(Rm) and E(ΔR(*t*) max). Figure 8 displays the scatter plot of RM versus the slope of the line drawn between E(Rm) and E(ΔR(*t*) max). The inferred preferential regression has $r = 0.97$ and $se = 11$, suggesting a slightly tighter fit than the fit for RM versus ΔR(*t*) max (fig. 2). Interesting is that all cycles having a slope larger than the median (2.25) at E(ΔR(*t*) max) have RM >114.9 and are fast-rising cycles, with 5 of 7 also being short-period cycles, while all cycles having a slope smaller than the median have RM < 114.9, with 6 of 7 being slow-rising cycles and 5 of 7 being long-period cycles. Thus, the slope measured at E(ΔR(*t*) max) provides a strong indication of the size of the ongoing sunspot cycle (14 of 14 cycles), the quickness of its rise to maximum amplitude (13 of 14 cycles), and the likely duration of the cycle (10 of 14 cycles).

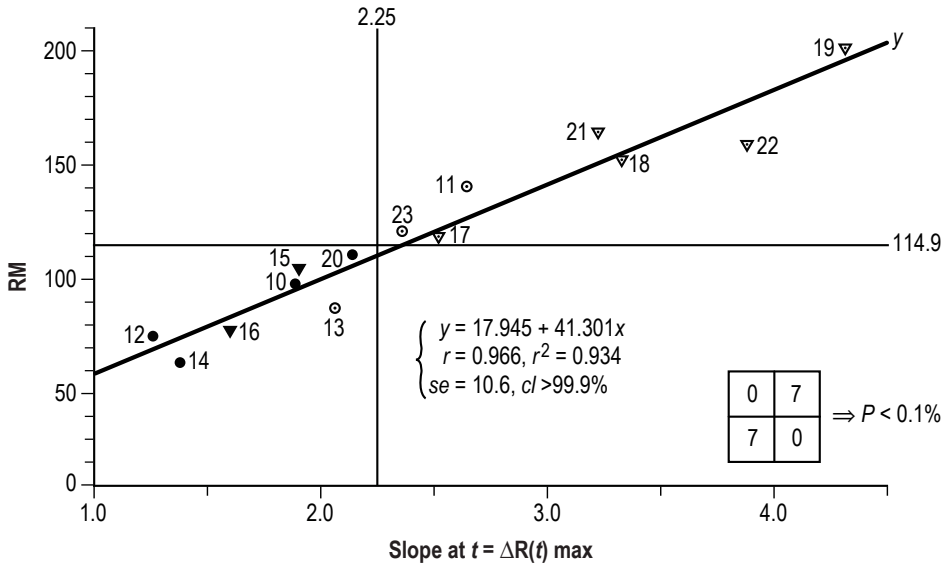

Figure 8. RM versus slope at $t = \Delta R(t)$ max.

Unfortunately, one does not know precisely when $\Delta R(t)$ max occurs until it actually has been observed. Instead, one can only monitor the month-to-month changes, applying the values in the formulations of figures 2 and 8 to deduce possible values for RM. Table 4 summarizes (a) the observed $R(t)$ values for cycles 10–23 for $t = 18$–32 mo and (b) the resultant slopes, and table 5 provides the statistical parameters associated with fits of RM versus $R(t)$. For comparison, the R(18) value and its associated slope for cycle 24 is included in table 4. Plainly, cycle 24's R(18) value (16.4) and associated slope (0.82) are the smallest on record. Applying the R(18) value in the inferred regression for R(18) values, one computes RM for cycle 24 to be about 74 ± 26.

Table 4. Values of $R(t)$ for $t = 18$–30 mo and slopes.

a. R(*t*) Values																	
Cycle	Rm	RM	R(18)	R(19)	R(20)	R(21)	R(22)	R(23)	R(24)	R(25)	R(26)	R(27)	R(28)	R(29)	R(30)	R(31)	R(32)
10	3.2	97.9	21.5	23.8	26.0	29.4	32.7	34.3	36.0	38.6	41.7	44.8	48.5	51.5	53.6	56.7	60.7
11	5.2	140.5	45.8	47.1	50.5	56.9	61.4	64.6	68.0	69.4	70.1	72.4	74.6	77.6	84.3	93.8	101.7
12	2.2	74.6	31.3	32.8	34.4	36.8	39.5	41.6	43.6	47.0	49.7	49.6	49.9	51.8	53.5	54.6	55.6
13	5.0	87.9	45.3	50.0	53.7	56.5	58.4	62.0	65.2	66.4	68.1	71.0	73.2	73.4	73.9	75.3	76.3
14	2.6	64.2	25.4	26.6	27.9	29.6	31.4	33.5	35.5	37.7	39.7	41.1	41.5	41.6	42.9	46.4	49.8
15	1.5	105.4	34.8	38.9	42.3	45.3	46.9	48.3	49.8	51.5	53.9	56.9	58.6	57.8	55.6	54.0	53.7
16	5.6	78.1	27.1	29.3	32.6	35.9	40.9	47.2	51.8	55.6	57.7	58.9	60.9	62.6	64.1	65.1	65.2
17	3.4	119.2	22.0	25.6	29.9	34.2	37.9	42.0	46.5	51.3	55.0	57.2	59.0	62.2	65.9	68.8	72.5
18	7.7	151.8	38.6	43.9	48.1	52.1	56.0	60.6	67.0	72.9	76.8	81.4	88.6	95.3	100.2	104.3	109.6
19	3.4	201.3	64.4	73.0	81.0	88.8	98.5	109.3	118.7	127.4	136.9	145.5	149.6	151.5	155.8	159.6	164.3
20	9.6	110.6	37.4	40.7	44.7	50.3	56.7	63.1	67.6	70.2	72.7	75.0	78.8	82.2	84.6	87.5	91.3
21	12.2	164.5	56.9	61.3	64.5	69.6	76.9	83.2	89.3	97.4	104.0	108.4	111.1	113.3	117.7	123.7	130.9
22	12.3	158.5	71.3	77.5	83.8	93.7	104.3	113.7	121.2	125.3	130.4	137.6	142.0	145.0	149.7	153.5	156.9
23	8.0	120.8	35.0	39.0	43.7	48.9	53.4	56.5	59.4	62.5	65.4	67.8	69.5	70.5	73.0	77.9	82.6
24	1.7	–	16.4														

Table 4. Values of R(t) for t = 18–30 mo and slopes. (Continued)

b. Slopes															
Cycle	**R(18)**	**R(19)**	**R(20)**	**R(21)**	**R(22)**	**R(23)**	**R(24)**	**R(25)**	**R(26)**	**R(27)**	**R(28)**	**R(29)**	**R(30)**	**R(31)**	**R(32)**
10	1.02	1.08	1.14	1.25	1.34	1.35	1.37	1.42	1.48	1.54	1.62	1.67	1.68	1.73	1.80
11	2.26	2.21	2.27	2.46	2.55	2.58	2.62	2.57	2.50	2.49	2.48	2.50	2.64	2.86	3.02
12	1.62	1.61	1.61	1.65	1.70	1.71	1.73	1.79	1.83	1.76	1.70	1.71	1.71	1.69	1.67
13	2.24	2.37	2.44	2.45	2.43	2.48	2.51	2.46	2.43	2.44	2.44	2.36	2.30	2.27	2.23
14	1.27	1.26	1.27	1.29	1.31	1.34	1.37	1.40	1.43	1.43	1.39	1.34	1.34	1.41	1.48
15	1.85	1.97	2.04	2.09	2.06	2.03	2.01	2.00	2.02	2.05	2.04	1.94	1.80	1.69	1.63
16	1.19	1.25	1.35	1.44	1.86	1.81	1.93	2.00	2.00	1.97	1.98	1.97	1.95	1.92	1.86
17	1.03	1.17	1.33	1.47	1.57	1.68	1.80	1.92	1.98	1.99	1.99	2.03	2.08	2.11	2.16
18	1.72	1.91	2.02	2.11	2.20	2.30	2.47	2.61	2.66	2.73	2.89	3.02	3.08	3.12	3.18
19	3.39	3.66	3.88	4.07	4.32	4.60	4.80	4.96	5.13	5.26	5.22	5.11	5.08	5.04	5.03
20	1.54	1.64	1.76	1.94	2.14	2.33	2.42	2.42	2.43	2.42	2.47	2.50	2.50	2.51	2.55
21	2.48	2.58	2.62	2.73	2.94	3.09	3.21	3.41	3.53	3.56	3.53	3.49	3.52	3.60	3.71
22	3.28	3.43	3.58	3.88	4.18	4.41	4.54	4.52	4.54	4.64	4.63	4.58	4.58	4.55	4.52
23	1.50	1.63	1.79	1.95	2.06	2.11	2.14	2.18	2.21	2.21	2.20	2.16	2.17	2.25	2.33
24	0.82														

Note: Slope is computed as [R(t) – Rm]/t.

Table 5. Statistical parameters for the RM versus R(t) fits for t = 18–32 mo.

t	*r*	*r*×*r*	*a*	*b*	*se*	*cl* (%)
18	0.771	0.595	41.327	1.970	26.123	99.8
19	0.796	0.633	39.255	1.847	24.887	99.9
20	0.814	0.662	36.751	1.751	23.815	99.9
21	0.826	0.683	35.872	1.611	23.214	99.9
22	0.834	0.695	37.156	1.453	22.711	99.9
23	0.833	0.694	39.227	1.310	22.637	99.9
24	0.843	0.711	39.202	1.225	22.085	99.9
25	0.860	0.740	37.122	1.187	21.039	99.9
26	0.869	0.755	37.263	1.129	20.260	99.9
27	0.875	0.765	38.601	1.063	19.932	99.9
28	0.883	0.779	37.405	1.041	19.457	99.9
29	0.892	0.795	35.557	1.036	18.677	99.9
30	0.901	0.812	35.008	1.009	17.737	99.9
31	0.911	0.830	33.203	0.991	16.997	99.9
32	0.922	0.850	31.656	0.969	16.059	99.9

3. DISCUSSION AND SUMMARY

The term 'sunspot cycle' refers to the quasi-periodic waxing and waning of sunspots over decadal time. While sunspots have been viewed telescopically since Galileo, the existence of the sunspot cycle itself has been recognized as being a real feature of the Sun only since the early-to-mid 1800s.[28–32] Sunspot cycles are numbered sequentially from minimum amplitude to minimum amplitude, with the present sunspot cycle being number 24 (this numbering based on the reconstruction performed by Rudolf Wolf[33]), having had its minimum amplitude in December 2008. At present, cycle 24 is in its rising phase towards maximum amplitude, which for the modern era sunspot cycles has followed minimum amplitude by 3–5 yr, dependent upon the strength of the cycle (strong cycles peaking earlier than weak cycles). Following maximum amplitude, which really is better described as a period of several years of enhanced solar activity rather than a specific point in time, the activity level will slowly subside until a level once again indicative of minimum amplitude is encountered. At minimum, a 1- to 3-yr overlap of old and new cycle spots[34] typically is seen, with the old cycle spots at low solar latitudes and the new cycle spots at higher solar latitudes (≥30 deg; see Wilson and Hathaway[24]).

Since the Maunder minimum of the late 1600s (a prolonged interval of time of several decades when few sunspots were reported), there has been a general upward secular increase with time in solar activity.[1,35] While other Maunder-like minima have been proposed, like the Dalton minimum (cycles 5 and 6, in the early 1800s) and the Modern minimum (cycles 12–14, in the late 1800s to early 1900s), the overall trend since the Maunder minimum has been generally upward, with a broad peak believed to have occurred about cycles 18–22 (the so-called Modern maximum, the mid-to-late 1900s). The trend in solar activity now, however, appears to be in decline, since cycle 23 was smaller than cycle 22, which also was smaller than cycle 21 (at least, in terms of 12-mma values of R).

Predictions for the size (and timing) of cycle 24 based on a variety of techniques,[36] including precursor, climatological, dynamo, neural network, and spectral models, have resulted in a wide range of values, from the very small to the very large. Obviously, some of these predictions will be deemed crudely successful, while others will fail miserably, thereby, leading, perhaps, to a better understanding of the physics involved in the generation of the solar cycle[37–40] and more accurate prediction of future sunspot cycles.

In this TP, the size and timing of cycle 24 has been estimated based on its early cycle behavior and application of the HWR shape-fitting function.[25] It is apparent that cycle 24 seems destined to be a cycle weaker in strength than was seen in cycle 23, which had RM = 120.8. If true, then the apparent downward trend in solar activity that has been underway since about cycles 21 or 22 continues and, perhaps, will result in the occurrence of another minimum of sunspot activity (like that which occurred during the Maunder, Dalton, or Modern minima).

Cycle 24's early behavior through $t = 18$ mo has continued to fall well below the activity level associated with the mean of cycles 10–23. At $t = 18$ mo past minimum (recall that 12-mma values trail current calendar time by 6 mo), the ratio of cycle 24's 12-mma value of R to that of the mean cycle is 0.41, inferring that cycle 24 will have an RM less than half the size of the mean modern era sunspot cycle, or about 50, provided that the ratio remains the same through the occurrence of its maximum amplitude. Mitigating this, however, is the belief that the maximum rate of change in the month-to-month R values has not yet been seen, which, if true, suggests that a larger ratio (>0.41) and larger RM (>50) will be seen in the months ahead for cycle 24.

To date (through $t = 18$ mo), the maximum month-to-month rate of change (i.e., the fd) of R has been 1.7, occurring at $t = 14$ and 15 mo, just within the window of when one expects to observe $\Delta R(t)$ max. On average, $\Delta R(t)$ max occurs about $t = 28$ mo past minimum amplitude, with 7 of 14 modern era cycles having $\Delta R(t)$ max occurring between $t = 14$ and 24 mo and 7 of 14 modern era cycles having $\Delta R(t)$ max occurring between $t = 30$ and 42 mo. The value of 1.7 for $\Delta R(t)$ max suggests $RM = 45.9 \pm 21.3$ for cycle 24. However, because $\Delta R(t)$ max for cycle 24 probably has not yet occurred, a higher RM is expected. Indeed, the observed value of aam for cycle 24 (8.4) suggests a slightly higher RM for cycle 24, namely, $RM = 54.6 \pm 16.6$, with only a 1% chance that RM will exceed 100.5. The value of $RM = 55$ suggests $ASC = 54 \pm 5$ mo (from the regression based on all modern era sunspot cycle) or 59 ± 4 mo (using the regression that ignores the extreme cycles 14 and 19) for cycle 24. Therefore, it appears highly likely that cycle 24 ultimately will be described as a weak, slow-rising sunspot cycle, having RM smaller and ASC longer than was observed in preceding cycle 23, potentially, becoming the smallest and the slowest rising cycle of the modern era (comparable in size to cycle 14 and comparable in ascent duration to cycles 12 and 16), which would be consistent with the 'low' panel consensus prediction.[36,38,41–47]

Comparison of the early cycle 24 $R(t)$ behavior (through $t = 18$ mo) with the mean cycle curves for specific groupings of cycles (i.e., FRC, SRC, SPC, and LPC) certainly supports this belief. For all comparisons, $R(t)$ values for cycle 24 fall well below the mean cycle curves, being most divergent for FRC and SPC, again, suggestive that cycle 24 probably is a weak, slow-rising cycle that also is a long-period cycle. If true, then maximum amplitude for cycle 24 will occur after December 2012 and new cycle 25 will not begin until after December 2019.

Application of the HWR shape-fitting function to the early cycle behavior of cycle 24 suggests that its behavior is consistent with a sunspot cycle having $RM = 70$ and $ASC = 56$ mo. This initial projection can be improved upon once $\Delta R(t)$ max is observed (probably sometime in 2011), which should result in a more accurate estimation of RM.

REFERENCES

1. Hathaway, D.H.; Wilson, R.M.; and Reichmann, E.J.: "Group Sunspot Numbers: Sunspot Cycle Characteristics," *Solar Phys.*, Vol. 211, p. 357, 2002.

2. Usoskin, I.G.; and Mursula, K.: "New Standpoints in Long-Term Solar Cycle Evolution: A Review," *Proc. ISCS 2003 Sympos., 'Solar Variability as an Input to the Earth's Environment,'* Tatranská Lomnica, Slovakia, June 23–28, 2003, ESA SP-535, pp. 25–36, September 2003.

3. De Jager, C.: "Solar Forcing of Climate. 1: Solar Variability," *Space Sci. Rev.*, Vol. 120, p. 197, 2005.

4. Solanki, S.K.; Usoskin, I.G.; Kromer, B.; et al.: "Unusual Activity of the Sun during Recent Decades Compared to the Previous 11,000 Years," *Nature*, Vol. 431, p. 1084, 2004.

5. Hathaway, D.H.; and Wilson, R.M.: "What the Sunspot Record Tells Us about Space Climate," *Solar Phys.*, Vol. 224, p. 5, 2004.

6. Schween, R.: "Space Weather: The Solar Perspective," *lrsp-2006-2*, 2006.

7. Schüssler, M.: "Are Solar Cycles Predictable?" *Astron. Nach.*, Vol. 328, p. 1087, December 2007.

8. Pulkkinen, T.: "Space Weather: Terrestrial Perspective," *lrsp-2007-1*, 2007.

9. Haigh, J.D.: "The Sun and the Earth's Climate," *lrsp-2007-2*, 2007.

10. Usoskin, I.G.; Solanki, S.K.; and Kovaltsov, G.A.: "Grand Minima and Maxima of Solar Activity: New Observational Constraints," *Astron. Astrophys.*, Vol. 431, p. 301, 2007.

11. Usoskin, I.G.: "A History of Solar Activity over Millennia," *lrsp-2008-3*, 2008.

12. Usoskin, I.G.; and Mursula, K.: "Long-Term Solar Cycle Evolution: Review of Recent Developments," *Solar Phys.*, Vol. 218, p. 319, 2008.

13. Hathaway, D.H.: "Solar Cycle Forecasting," *The Origin and Dynamics of Solar Magnetism*, Springer, New York, p. 401, 2009.

14. Hathaway, D.H.: "The Solar Cycle," *lrsp-2010-1*, 2010.

15. Petrovay, K.: "Solar Cycle Prediction," *lrsp-2010-6*, 2010.

16. Wilson, R.M.; and Hathaway, D.H.: "Using the Inflection Points and Rates of Growth and Decay to Predict Levels of Solar Activity," *NASA/TP—2008–215473*, Marshall Space Flight Center, AL, <http://trs.nis.nasa.gov/archive/00000787/>, September 2008.

17. Ohl, A.I.: "Wolf's Number Prediction for the Maximum of the Cycle 20," *Solnice Danie*, No. 12, p. 84, 1966.

18. Ohl, A.I.: "A Preliminary Forecast of Some Parameters of Cycle No. 21 of the Solar Activity," *Solnice Danie*, No. 9, p. 73, 1976.

19. Wilson, R.M.; and Hathaway, D.H.: "Using the Modified Precursor Method to Estimate the Size of Cycle 24," *NASA/TP—2008–215467*, Marshall Space Flight Center, AL, <http://trs.nis.nasa.gov/archive/00000789/>, July 2008.

20. Wilson, R.M.; and Hathaway, D.H.: "Predicting the Size of Cycle 24 on the Basis of Single- and Bi-Variate Geomagnetic Precursor Methods," *NASA/TP—2009–215687*, Marshall Space Flight Center, AL, <http://trs.nis.nasa.gov/archive/00000799/>, February 2009.

21. Kane, R.P.: "Size of the Coming Solar Cycle 24 based on Ohl's Precursor Method," *Ann. Geophys.*, Vol. 28, p. 1463, 2010.

22. Wilson, R.M.: "Predicting the Size and Timing of Sunspot Maximum for Cycle 24," *NASA/TP—2010–216433*, Marshall Space Flight Center, AL, <http://trs.nis.nasa.gov/archive/00000828/>, June 2010.

23. Wilson, R.M.; Hathaway, D.H.; and Reichmann, E.J.: "On the Importance of Cycle Minimum in Sunspot Cycle Prediction," *NASA Technical Paper 3648*, Marshall Space Flight Center, AL, <http://trs.nis.nasa.gov/archive/00000335/>, August 1996.

24. Wilson, R.M.; and Hathaway, D.H.: "Sunspot Activity near Cycle Minimum and What It Might Suggest for Cycle 24, the Next Sunspot Cycle," *NASA/TP—2009–216061*, Marshall Space Flight Center, AL, <http://trs.nis.nasa.gov/archive/00000814/>, September 2009.

25. Hathaway, D.H.; Wilson, R.M.; and Reichmann, E.J.: "The Shape of the Sunspot Cycle," *Solar Phys.*, Vol. 151, p. 177, 1994.

26. Svalgaard, L.; Cliver, E.W.; and Kamide, Y.: "Sunspot Cycle 24: Smallest in 100 Years?" *Geophys. Res. Lett.*, Vol. 32, p. L01104, 2005.

27. Everitt, B.S.: *The Analysis of Contingency Tables*, John Wiley & Sons, New York, p. 14, 1977.

28. Schwabe, H.: "Sonnen-Beobachtungen im Jahre 1843," *Astron. Nach.*, Vol. 21, p. 233, 1844.

29. Kiepenheur, K.O.: "Solar Activity," in *The Sun*, G.P. Kuiper (ed.), The University of Chicago Press, Chicago, p. 322, 1953.

30. Bray, R.J.; and Loughhead, R.E.: *Sunspots*, John Wiley & Sons, New York, p. 4, 1964.

31. Hoyt, D.V.; and Schatten, K.H.: *The Role of the Sun in Climate Change*, Oxford University Press, New York, p. 34, 1997.

32. Eddy, J.A.: "The Historical Record of Solar Activity," in *The Ancient Sun: Fossil Record in the Earth, Moon and Meteorites*, R.O. Pepin, J.A. Eddy, and R.B. Merrill (eds.), Pergamon Press, New York, p. 119, 1980.

33. Waldmeier, M.: *The Sunspot-Activity in the Years 1610-1960*, Swiss Federal Observatory, Schulthess & Co., Zurich, p. 5, 1961.

34. Howard, R.: "2. Solar Cycle, Solar Rotation and Large-Scale Circulation," in *Illustrated Glossary for Solar and Solar-Terrestrial Physics*, A. Bruzek and C.J. Durrant (eds.), D. Reidel Publishing Co., Boston, p. 7, 1977.

35. Wilson, R.M.: "On the Long-Term Secular Increase in Sunspot Number," *Solar Phys.*, Vol. 115, p. 397, 1988.

36. Pesnell, W.D.: "Predictions of Solar Cycle 24," *Solar Phys.*, Vol. 252, p. 209, 2008.

37. Ossendrijver, M.: "The Solar Dynamo," *Astron. Astrophys. Rev.*, Vol. 11, p. 287, 2003.

38. Choudhuri, A.R.; Chatterjee, P.; and Jiang, J.: "Predicting Solar Cycle 24 with a Solar Dynamo Model," *Phys. Rev. Lett.*, Vol. 98, p. 131,103, 2007.

39. Hathaway, D.H.: "Solar Cycle Forecasting," *The Origin and Dynamics of Solar Magnetism*, M.J. Thompson et al. (eds.), *Space Sci. Rev.*, Vol. 32, p. 401, 2008.

40. Charbonneau, P.: "Dynamo Models of the Solar Cycle," *lrsp-2010-3*, 2010.

41. Schatten, K.H.: "Solar Activity and the Solar Cycle," *Adv. Space Res.*, Vol. 32, p. 451, 2003.

42. Duhau, S.: "An Early Prediction of Maximum Sunspot Number in Solar Cycle 24," *Solar Phys.*, Vol. 213, p. 203, 2003.

43. Sello, S.: "Solar Cycle Activity: A Preliminary Prediction for Cycle 24," *Astron. Astrophys.*, Vol. 410, p. 691, 2003.

44. Javaraiah, J.: "Predicting the Amplitude of a Solar Cycle Using the North-South Asymmetry in the Previous Cycle: II. An Improved Prediction for Solar Cycle 24," *Solar Phys.*, Vol. 252, p. 419, 2008.

45. Wilson, R.M.; and Hathaway, D.H.: On the Period-Amplitude and Amplitude-Period Relationships, *NASA/TP—2008–215580*, Marshall Space Flight Center, AL, <http://trs.nis.nasa.gov/archive/00000794/>, November 2008.

46. De Jager, C.; and Duhau, S.: "Forecasting the Parameters of Sunspot Cycle 24 and Beyond," *J. Atmos. Solar-Terr. Phys.*, Vol. 71, Issue 2, p. 239, February 2009.

47. Rigozo, N.R.; Souza Echer, M.P.; Evangelista, H.; et al.: "Prediction of Sunspot Number Amplitude and Solar Cycle Length for Cycles 24 and 25," *J. Atmos. Terr. Phys.*, in press, corrected proof, online September 2010.

REPORT DOCUMENTATION PAGE

Form Approved
OMB No. 0704-0188

1. REPORT DATE *(DD-MM-YYYY)*	2. REPORT TYPE	3. DATES COVERED *(From - To)*
01–03–2011	Technical Publication	

4. TITLE AND SUBTITLE

An Estimate of the Size and Shape of Sunspot Cycle 24 Based on Its Early Cycle Behavior Using the Hathaway-Wilson-Reichmann Shape-Fitting Function

5a. CONTRACT NUMBER

5b. GRANT NUMBER

5c. PROGRAM ELEMENT NUMBER

6. AUTHOR(S)

Robert M. Wilson

5d. PROJECT NUMBER

5e. TASK NUMBER

5f. WORK UNIT NUMBER

7. PERFORMING ORGANIZATION NAME(S) AND ADDRESS(ES)

George C. Marshall Space Flight Center
Marshall Space Flight Center, AL 35812

8. PERFORMING ORGANIZATION REPORT NUMBER

M–1310

9. SPONSORING/MONITORING AGENCY NAME(S) AND ADDRESS(ES)

National Aeronautics and Space Administration
Washington, DC 20546–0001

10. SPONSORING/MONITOR'S ACRONYM(S)

NASA

11. SPONSORING/MONITORING REPORT NUMBER

NASA/TP—2011–216461

12. DISTRIBUTION/AVAILABILITY STATEMENT

Unclassified-Unlimited
Subject Category 92
Availability: NASA CASI (443–757–5802)

13. SUPPLEMENTARY NOTES

Prepared by the Science and Exploration Research Office, Science and Mission Systems Office

14. ABSTRACT

On the basis of 12-month moving averages (12-mma) of monthly mean sunspot number (R), sunspot cycle 24 had its minimum amplitude (Rm = 1.7) in December 2008. At 12 mo past minimum, R measured 8.3, and at 18 mo past minimum, it measured 16.4. Thus far, the maximum month-to-month rate of rise in 12-mma values of monthly mean sunspot number ($\Delta R(t)$ max) has been 1.7, having occurred at elapsed times past minimum amplitude (t) of 14 and 15 mo. Compared to other sunspot cycles of the modern era, cycle 24's Rm and $\Delta R(t)$ max (as observed so far) are the smallest on record, suggesting that it likely will be a slow-rising, long-period sunspot cycle of below average maximum amplitude (RM). Supporting this view is the now observed relative strength of cycle 24's geomagnetic minimum amplitude as measured using the 12-mma value of the aa-geomagnetic index (aam = 8.4), which also is the smallest on record, having occurred at t equals 8 and 9 mo. From the method of Ohl (the inferred preferential association between RM and aam), one predicts RM = 55 ± 17 (the ±1 *se* prediction interval) for cycle 24. Furthermore, from the Waldmeier effect (the inferred preferential association between the ascent duration (ASC) and RM) one predicts an ASC longer than 48 mo for cycle 24; hence, maximum amplitude occurrence should be after December 2012. Application of the Hathaway-Wilson-Reichmann shape-fitting function, using an RM = 70 and ASC = 56 mo, is found to adequately fit the early sunspot number growth of cycle 24.

15. SUBJECT TERMS

Sun, sunspot cycle prediction, cycle 24, method of Ohl, Waldmeier effect, Hathaway-Wilson-Reichmann shape-fitting function, inflection points

16. SECURITY CLASSIFICATION OF:			17. LIMITATION OF ABSTRACT	18. NUMBER OF PAGES	19a. NAME OF RESPONSIBLE PERSON
a. REPORT	b. ABSTRACT	c. THIS PAGE			STI Help Desk at email: help@sti.nasa.gov
U	U	U	UU	32	19b. TELEPHONE NUMBER *(Include area code)* STI Help Desk at: 443–757–5802

National Aeronautics and
Space Administration
IS20
George C. Marshall Space Flight Center
Marshall Space Flight Center, Alabama
35812